

Report of the short-term scientific mission

Comparison of AOD calibration methods for Brewer spectrophotometers using a UV-PFR or a Brewer as reference

at AEMET/IARC, Santa Cruz, Tenerife,
performed by Thomas Carlund (PMOD/WRC, Davos, Switzerland)

Abstract

To compare calibration methods, and in the end retrieved aerosol optical depth (AOD), for Brewer spectrophotometers Thomas Carlund (PMOD) visited AEMET/IARC, Santa Cruz, Tenerife, for a short term scientific mission within the COST ES1207 EUBREWNET project. The STSM visit was made during 4-8 April 2016.

Of great importance to retrieved AOD values is how the many calculated input parameters are derived. Consequently, the algorithms and coefficients used by the groups at IARC and PMOD were reviewed and the effect of several identified differences was quantified. These results led to changes both in the IARC and PMOD AOD retrievals which now harmonize better with each other.

For reference instruments it is important to apply a correct Langley calibration method, as well as correct the Brewers for internal polarization effects in the Langley plot calibrations. For the UV-PFR sunphotometer, used as reference instrument by PMOD, the influence of the 1.0 – 1.3 nm wide FWHMs need to be corrected for. With the use of adequate calibration methods and taking necessary corrections into account, calibration results for Brewer #185 from Langley plots at Izaña, analysed independently by the two groups, and calibration against the UV-PFR#1001 at the 10th RBCC-E campaign, agreed within ± 1 % from each other. And as a result of this, also AOD values determined for a field Brewer by the two groups agreed well with each other. It is concluded that Brewer #185 and UV-PFR#1001 both provided valid AOD calibrations at the 10th RBCC-E campaign.

What still remains uncertain in the Brewer AOD retrievals is how to correct for internal polarization effects, both at high and low solar zenith angles, and how to derive and apply corrections for temperature dependence of (absolute) irradiance measurements.

Introduction

The absorption and scattering of solar radiation by aerosols has been recognized as an important parameter for climate forcing studies. Furthermore, the absorption of surface ultraviolet (UV) radiation by aerosols has also become of major interest because of the harmful effects of UV radiation on Humans and more generally on the biosphere. Especially in heavily polluted areas, the decrease of UVB radiation due to the absorption of aerosols can become larger than the expected increase of UV radiation due to the declining ozone levels. Thus, the determination of aerosol properties, especially the aerosol optical depth (AOD) in the UV wavelength region is of great importance to understand the climatological variability of UV radiation. Retrieval of aerosol optical depth (AOD) in the UV from the European Brewer Network is therefore one of the three main objectives of COST Action ES1207. This will both extend routine AOD observations to a new wavelength range and to some new sites without aerosol measurements today. To derive AOD from Brewer measurements the instruments need to be specifically calibrated for this purpose. Currently, this is not part of the standard procedures for e.g. ozone calibrations.

Aerosol optical depth from Brewer spectrophotometers have been studied by several groups (e.g. Bais, 1997; Cheymol and De Backer, 2003; Cheymol et al., 2006; Marenco et al., 2002; Gröbner and Meleti, 2004; Kazadzis et al. 2007; Kumharn et al., 2012). The necessary absolute calibration for AOD has mostly been done using some Langley-plot technique, which currently is regarded as the best method if performed at a high altitude site with low and stable aerosol load as well as stable (total column) ozone conditions. Alternatively, calibration has been made against lamp, or through combination of sun and lamp measurements. For a station network, such as the EUBREWNET, it is not feasible to calibrate all field instruments by some Langley-plot method. Also there is no common and relatively easy high accuracy lamp calibration of the direct sun measurements available.

The aim here is to utilize calibration campaigns such as the RBCC-E campaigns for ozone and UV to also calibrate the Brewers for AOD. At these campaigns there are/could be reference instruments available which have absolute Langley calibrations from a suitable high altitude site. Currently, there are two reference AOD instruments available for the EUBREWNET, Brewer #185 and the UV-PFR#1001 sunphotometer. With the relatively simple and robust instrument such as the UV-PFR it is also planned to perform station visits, as another way transfer AOD calibration to field sites.

While all Brewers are measuring at the same wavelengths and with approximately the same bandwidth (FWHM), the UV-PFR measures at slightly different UV wavelengths and with wider FWHM. Due to this fact, the methods of AOD calibrations might be different depending on which instrument will be used as reference. Hence, the main focus of this STSM is a comparison of calibration methods and the results using different reference instruments for absolute calibration of Brewer spectrophotometers. For this work it is natural to start with a review of the various algorithms and spectral data sets (solar zenith angle, air mass components, Rayleigh optical depth, ozone absorption coefficients, etc.) used for the input parameters needed in the AOD calculations.

Algorithms and coefficients

From the Beer-Bouguer-Lambert law, the spectral aerosol optical depth ($AOD = \delta_a$) at wavelength λ is calculated as

$$AOD_\lambda = \delta_{a,\lambda} = \ln\left(\frac{I_{0,\lambda}}{R^2 I_\lambda}\right) / m_a - \frac{m_R p}{m_a p_0} \delta_{R,\lambda} - \frac{m_o}{m_a} \delta_{o,\lambda} \quad (1)$$

from the measurements of the spectral irradiance I_λ . The $I_{0,\lambda}$ are the calibration constants of the instrument and equals the values that would have been measured with the instrument above the atmosphere at mean Sun-Earth distance. R is the actual Sun-Earth distance expressed in AU. The (relative) optical air mass terms m_a , m_R and m_o are the optical air masses of the aerosol extinction, Rayleigh scattering and ozone absorption, respectively. (In the following, mostly just the term air mass will be used instead of optical air mass.¹) Air pressure, p , is the pressure at the station level and $p_0 = 1013.25$ hPa is the standard pressure at sea-level. The ozone optical depth, $\delta_{o,\lambda}$, is calculated from ozone absorption coefficient $k_{o,\lambda}$ and the total column ozone TCO as $\delta_{o,\lambda} = k_{o,\lambda} \cdot TCO$. The ozone absorption coefficients are derived from laboratory measurements of ozone cross sections and possibly also corrected for effective ozone layer temperature. The ozone amount is preferably taken from collocated measurements with a Brewer or Dobson spectrophotometer.

As an example of the effective ozone temperature, climatological effective ozone temperature calculated from the “ML-climatology” (McPeters and Labow, 2012) is shown in figure 1. Also effective ozone layer altitude varies in time and space and climatological values of the altitude is also shown in figure 1. The simplified method for calculating the effective ozone temperature is given in e.g. Redondas et al. (2014).

1) Definition according to AMS Glossary: optical air mass—(Originally called air mass.) A measure of the length of the path through the atmosphere to sea level traversed by light rays from a celestial body, expressed as a multiple of the pathlength for a light source at the zenith.

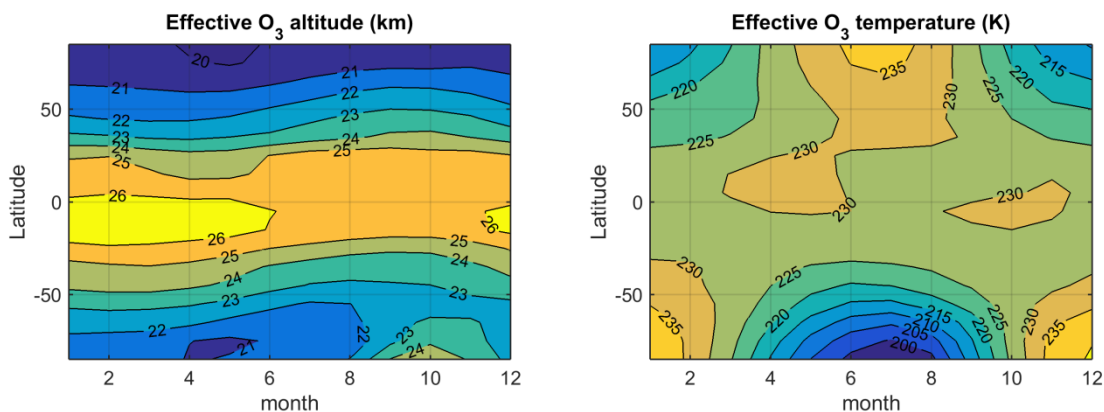


Figure 1. Effective ozone altitude (left) and effective ozone temperature (right) calculated from the “ML-climatology” 1988-2010.

Table 1. Algorithms and coefficients used in operational Brewer and UV-PFR measurements.

Parameter	BREWER		UV-PFR	
	Input variable(s)	Reference	Input variable(s)	Reference
Sun-Earth distance, R	Daynumber	Iqbal (1983)	Date and time	Michalsky (1988), w. Errata.
True and apparent solar zenith angle, SZA_t and SZA_a	Latitude, longitude, date, time.	Brewer operational software	Latitude, longitude, station altitude, date, time, air pressure, annual mean 2-m temperature at station	Reda & Andreas (2003), revised 2008.
Rayleigh airmass, m_R	SZA_t , layer height = 5 km	Brewer operational software	SZA_a	Kasten & Young (1989)
Rayleigh optical depth, $\delta_{R,\lambda}$	Wavelength	Standard coefficients used in Brewer operational software	Wavelength, pressure, station altitude, latitude	Bodhaine et al. (1999)
Aerosol airmass, m_a	$m_a = m_R$		SZA_a	Gueymard (1995). (Same as m_{water})
Effective ozone altitude and temperature, $O3_{alt}$, $O3_T$	$O3_{alt} = 22 \text{ km}$, $O3_T = -45 \text{ }^\circ\text{C}$			"ML-climatology" 1988-2010. McPeters and Labow (2012). ftp://toms.gsfc.nasa.gov/pub/ML_climatology/
Ozone airmass, m_o	SZA_t , $O3_{alt}$. Station altitude = 0 km (for all sites).	Brewer operational software	Latitude, date	
Ozone absorption coefficients (cross sections), $k_{o,\lambda} = L * O3_{XS}$			SZA_t , $O3_{alt}$, station altitude	Komhyr, et al. (1989)
Ozone amount, TCO (DU)	Wavelength, slit function	Bass & Paur, 1985. (T=-45 degC)	Wavelength, spectral response function, $O3_T$ (only for Serdyuchenko et al. O_3_{XS})	Bass & Paur, 1985. (T=-45 degC) or Serdyuchenko, et al. (2011), Temperature quadratic fit coefficients.
Ozone optical depth, $\delta_{o,\lambda}$	From Brewer DS measurement			Measured by collocated Brewer
	$k_{o,\lambda}$, TCO	$\delta_{o,\lambda} = k_{o,\lambda} * TCO / 1000$	$k_{o,\lambda}$, TCO	$\delta_{o,\lambda} = k_{o,\lambda} * TCO / 1000$

Table 2. Dependence of effective ozone layer height with latitude. From Operations handbook – ozone observations with a Dobson spectrophotometer (WMO, 2008).

Station Latitude, ϕ in degrees	Height h of Ozone Layer Above Mean Sea Level in Km
± 0	26
± 10	25
± 20	24
± 30	23
± 40	22
± 50	21
± 60	20
± 70	19
± 80	18
± 90	17

Another climatology of effective ozone altitude used for ozone measurements with Dobson spectrophotometers is given by WMO (2009), shown in table 2. Especially at higher latitudes, there is a relatively large difference between the climatologies for effective ozone layer altitude.

There exist several different ways to determine the optical depth and air mass terms on the right-hand side of equation 1. Table 1 lists the algorithms, coefficients and references for the AOD calculation currently used for Brewer spectrophotometers and the UV-PFR sunphotometer, respectively.

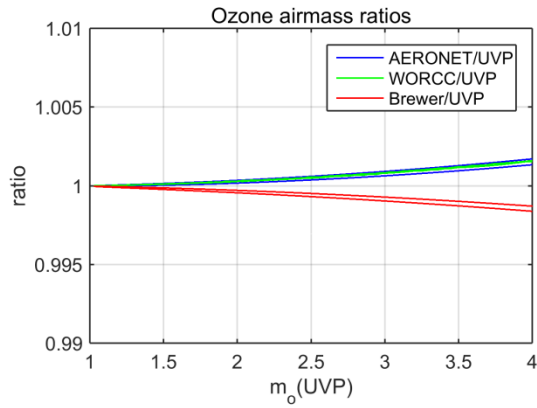
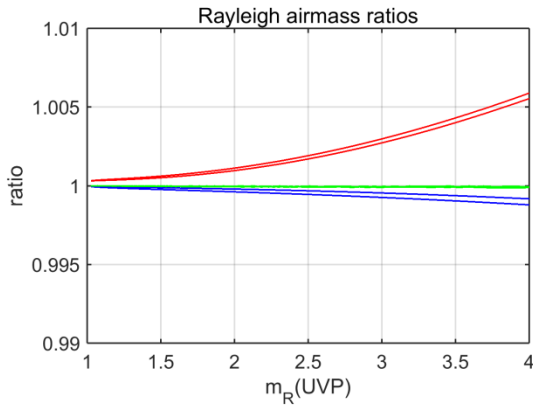
Potential absorption in NO_2 and SO_2 is not included in equation 1. The actual amounts of these gases over the measurement site(s) are generally not known and are here assumed to be negligibly small.

Since the various algorithms and coefficients gives slightly different results a brief comparison of the algorithms and coefficients used for the Brewers and the UV-PFR is made below. Also values used by AERONET and at WORCC (World Optical Depth Research and Calibration Centre) for the WMO/GAW global network of PFR sunphotometers are included in some cases

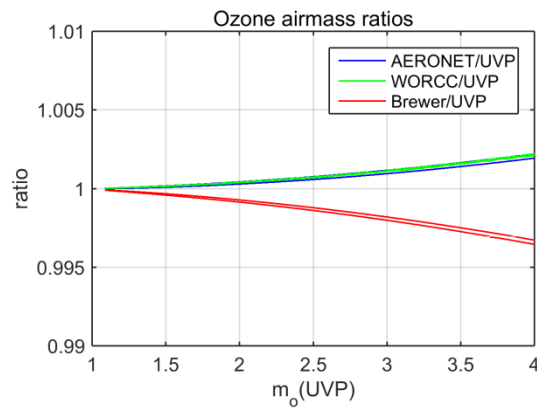
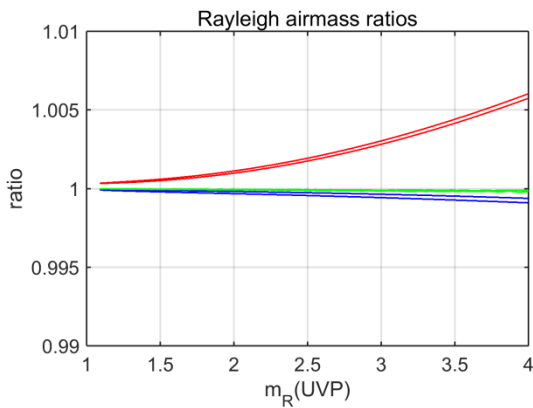
Air mass algorithms

The methods of calculating the air mass terms for the Brewers and the UV-PFR are listed in table 1. In the left column of figure 2, the ratio of different m_R over the m_R used for the UV-PFR are shown for some example days at the sites Izaña (IZO), Davos (DAV) and Sodankylä (SOD). The operational calculation of Rayleigh air mass in the Brewer overestimates m_R compared to the m_R calculations according to Kasten and Young (1989) which is used by the AERONET and at WORCC for the GAW/PFR global network, as well as for the UV-PFR. The overestimation is very similar at all sites and at all times of the year and varies from zero at air mass 1 to near +0.4% at air mass 3. The m_R results are very similar for AERONET, WORCC and UV-PFR since they use the same m_R formula. What differs is the algorithm to calculate solar position. The small differences in solar elevation/zenith angle (generally within $\pm 0.01^\circ$ in the studied air mass range, $m < 4$) do not result in any significant difference in the Rayleigh air mass term between these networks. For the EUBREWNET database it may be considered to update the formula for m_R to the one by Kasten & Young (1989) which is considered more accurate. The Brewer zenith angle calculations need not to be changed.

Ratio of different Rayleigh airmasses, IZO 2014-05-01.



Ratio of different Rayleigh airmasses, DAV 2014-06-21.



Ratio of different Rayleigh airmasses, SOD 2011-05-21.

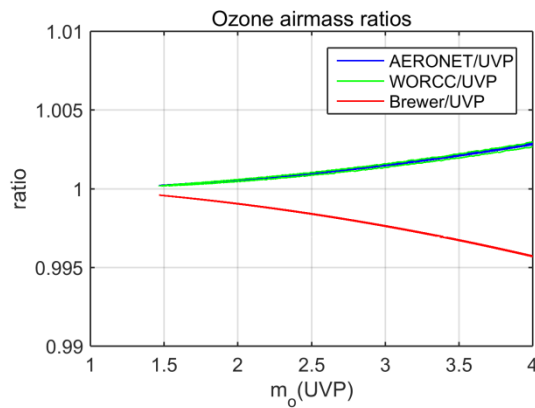
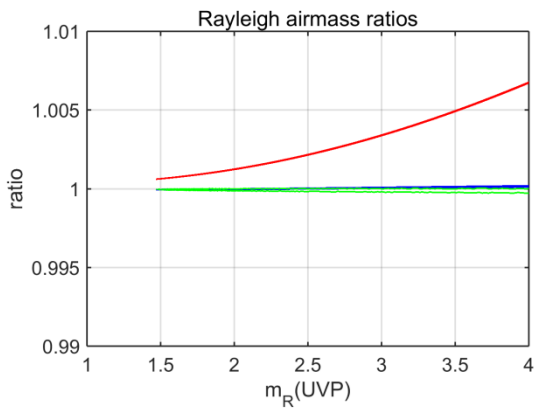


Figure 2. Comparison of Rayleigh (left column) and ozone (right column) air mass calculations during some example days at the stations Izaña, Davos and Sodankylä. The ratios shown are $m_{R,i}/m_{R,ref}$. The reference $m_{R,ref}$ is here taken as the m_R of the UV-PFR calculations. The principle is the same for the m_o ratios. The legend is the same for both Rayleigh and ozone air mass results.

The difference in ozone air mass calculations is more varying primarily dependent on the different effective ozone altitude in use. The fact that station altitude is not taken into account in the operational Brewer calculations has a negligible effect on the resulting AOD, at least in the air mass range considered here.

In an attempt to quantify the effect on derived AOD using different air mass algorithms or different input to the algorithms, the resulting change in AOD for typical measurement conditions during the 10th RBCC-E campaign, El Arenosillo 2015, using Bass and Paur (1985) ozone coefficients are given in table 3.

Table 3. Effects on AOD of various errors or different input to calculations of AOD.

Algorithm/coefficient difference	Effect on AOD (Conditions: $1 < m < 3$, at sea level, $AOD_{320} \approx 0.23$ TCO around 350 DU.)	
Using $m_a = m_R$ for a case when the true aerosol airmass is described by $m_a = m_w$	0 to +0.001, all UV wavelengths, slightly dependent on air mass.	
Using m_R according to operational Brewer algorithm, including $m_a = m_R$	0 to -0.0025, dependent on air mass, slightly dependent on λ .	
Using m_o calculated for ozone altitude of 22 km when the true altitude is 19 km	0 to -0.007 for $\lambda = 306.3$ nm 0 to -0.001 for $\lambda = 320.0$ nm Dependent on air mass and ozone amount. The influence is weaker and of opposite sign if the true altitude is 25 km.	
Using $p = 1000$ hPa instead of the correct values 1020 hPa or 980 hPa	$\lambda = 306.3$ nm: +0.022 for true pressure=1020 hPa -0.022 for true pressure=980 hPa $\lambda = 320.0$ nm: +0.018 for true pressure=1020 hPa -0.018 for true pressure=980 hPa	
Using default Brewer Rayleigh coefficients and correct p (See also table 4.)	-0.0083 for $\lambda = 306.3$ nm -0.0074 for $\lambda = 320.0$ nm Tiny reduction with increasing airmass	
Using default Brewer Rayleigh in ozone determination at El Arenosillo, resulting in 3 DU too high TCO	Brewer -0.0123 for $\lambda = 306.3$ nm -0.0069 for $\lambda = 310.05$ nm -0.0047 for $\lambda = 313.5$ nm -0.0026 for $\lambda = 316.8$ nm -0.0020 for $\lambda = 320.0$ nm Dependent on TCO	UV-PFR -0.0134 for $\lambda = 305.3$ nm -0.0061 for $\lambda = 311.3$ nm -0.0026 for $\lambda = 317.5$ nm -0.0002 for $\lambda = 332.3$ nm
Using ozone cross sections from Serdyuchenko, et al. (2011), compared to Bass and Paur (1985), both for -45 °C (See also tables 3 and 4.)	Brewer -0.0094 for $\lambda = 306.3$ nm -0.0028 for $\lambda = 310.05$ nm -0.0021 for $\lambda = 313.5$ nm +0.0019 for $\lambda = 316.8$ nm -0.0026 for $\lambda = 320.0$ nm Dependent on TCO	UV-PFR -0.0229 for $\lambda = 305.3$ nm -0.0047 for $\lambda = 311.3$ nm +0.0008 for $\lambda = 317.5$ nm -0.0017 for $\lambda = 332.3$ nm

For the small air mass range considered ($m \leq 3$) the effect of using $m_o = m_R$ for a case during the El Arenosillo campaign is very small. The error increases at higher air masses, $m > 3$, which are used for AOD determinations at UVA-NIR wavelengths. The effect of using the operational Rayleigh air mass calculation for the Brewers compared to using the common formula by Kasten and Young (1989) is a bit stronger but still fairly small, up to about -0.0025 at air mass 3.

Especially according to the effective ozone altitude used in the calculation of ozone from Dobson spectrophotometers, the ozone altitude decreases markedly towards higher latitudes. For a case when the default value of 22 km is used instead of a true effective ozone altitude of 19 km the AOD at the shortest wavelength (306.3 nm) is underestimated by 0.005 at $m_o = 3$. The error increases with increasing ozone amount. Due to the strongly decreasing ozone absorption the effect is negligible at the longest wavelength (320.0 nm), at least for $m_o \leq 3$ and $TCO \leq 350$ DU.

Rayleigh optical depth and ozone absorption coefficients

Both for the measurement of AOD as well as in calibration of instrument to measure UV AOD the Rayleigh scattering coefficients (optical depths) and the ozone absorption coefficients in use are influencing the result. Rayleigh optical depths (δ_R) and ozone absorption coefficients (k_o) that are or could be used in calculation of AOD from measurements with the UV-PFR#1001 and a Brewer spectrophotometer are listed in tables 4 and 5. To start with, the impact on AOD retrievals of the different versions of Rayleigh coefficients will be quantified in the following.

An algorithm to calculate the Rayleigh optical depth, which is considered accurate, has been developed by Bodhaine et al. (1999). Their comprehensive algorithm takes into account e.g. the latitudinal change in the acceleration of gravity and atmospheric CO_2 concentration. The δ_R results calculated with the Bodhaine et al. algorithm which are listed in tables 4 and 5 were calculated for the El Arenosillo site and a CO_2 concentration of 400 ppm. Clearly, the operational values of δ_R used in the Brewer calculations differ significantly from the values calculated according to Bodhaine et al. (1999). This results in underestimated AOD by more than 0.008 at the shortest Brewer wavelength (table 2). For a high latitude site such as Sodankylä, Finland, the accumulated negative bias in AOD can exceed -0.015 due to erroneous Rayleigh coefficients, default effective ozone altitude of 22 km and using the operational formula for m_R in the Brewers.

The potentially largest error in the Rayleigh correction term for the Brewers comes from the fact that a constant value of the station air pressure is used. For example, with a true station pressure deviating +20 hPa (-20 hPa) from the climatological constant value in use, which regularly occurs at mid to high latitudes, the AOD is overestimated (underestimated) by 0.022 at the shortest wavelength. The error decreases to 0.018 at the longest wavelength (320.0 nm).

Due to the narrow and symmetrical shape of the Brewer slit functions around their central wavelengths, convolving high spectral resolution Rayleigh optical depth with the slit functions has no significant effect on the resulting Rayleigh optical depths to be used. Even when also convolving with a high resolution extra-terrestrial solar spectrum the effect on δ_R is ≤ 0.0003 for the Brewer wavelengths. Due to the wider and slightly less symmetrical shape of the UV-PFR's filter functions, convolving the Rayleigh optical depth with the filter functions results in slightly higher differences than for the Brewer. However, the effect of also convolving with an extra-terrestrial solar spectrum decreased the differences to nearly zero for the UV-PFR. As a consequence, both for the Brewer and

the UV-PFR the Rayleigh optical depths can be calculated for the effective central wavelengths without any convolution.

All brewer spectrophotometers are very similar in wavelength. For this reason the same general wavelengths are used for all Brewers in the (first) AOD calibrations versus the UV-PFR. However, in reality there are small differences in the wavelengths between Brewers. Redondas et al. (2014) list average and standard deviation of 123 wavelength calibrations on 33 instruments done by the RBCC-E (Regional brewer Calibration Center - Europe). The average wavelengths are the same as are used here (table 5) and the standard deviation was <0.02 nm for all wavelengths. The Rayleigh optical depth coefficients for a Brewer slit which differs by two standard deviations from the mean/general value differ by less than 0.001 in optical depth from the value at the mean wavelength.

For the total column ozone determination with a Brewer, using the default/operational Brewer Rayleigh coefficients also results in a slight overestimation of the measured ozone amount. For the El Arenosillo campaign the “official” TCO was overestimated by about 3 DU due to the use of the default Rayleigh coefficients for the Brewer. This has a strong impact on the retrieval of AOD at the short wavelengths. For the shortest UV-PFR and Brewer wavelengths AOD is underestimated by more than 0.013 and 0.012, respectively. Errors at the other wavelengths are given in table 3.

Table 4. Rayleigh optical depth and ozone absorption coefficients for the UV-PFR#1001. The example ozone optical depth in the last column is calculated for the Bass&Paur absorption coefficients and an ozone amount of 350 DU.

Channel (nm)	Convolved effective central wavelength (nm)	δ_R Bodhaine (1999)	k_o B&P (-45°C) cm^{-1}	k_o IUP QFT (-45°C) cm^{-1}	k_o IUP 5dig (-45°C) cm^{-1}	δ_o B&P (-45°C, 350 DU)
305	305.31	1.1287	4.4682	4.5336	4.5199	1.5639
311	311.34	1.0377	2.0362	2.0497	2.0574	0.7127
318	317.50	0.9542	0.8802	0.8778	0.8819	0.3081
332	332.32	0.7856	0.0597	0.0645	0.0645	0.0209

Table 5. Rayleigh optical depth and ozone absorption coefficients for a general Brewer spectrophotometer. The example ozone optical depth in the last column is calculated for the Bass&Paur absorption coefficients and an ozone amount of 350 DU.

General Brewer wavelengths (nm)	δ_R Bodhaine (1999)	δ_R Brewer operat.	k_o B&P (-45°C) cm^{-1}	k_o IUP QFT (-45°C) cm^{-1}	k_o IUP 5dig (-45°C) cm^{-1}	δ_o B&P (-45°C, 350 DU)
306.30	1.1131	1.1214	4.1118	4.1387	4.1339	1.4391
310.05	1.0564	1.0638	2.3071	2.3150	2.3174	0.8075
313.50	1.0074	1.0154	1.5508	1.5568	1.5667	0.5428
316.80	0.9633	0.9717	0.8644	0.8590	0.8619	0.3025
320.00	0.9227	0.9302	0.6721	0.6796	0.6821	0.2352

Several results of laboratory measurements of ozone cross sections are available. Here, cross section data sets from only two sources have been investigated. For the current operational ozone determinations from Brewer measurements the cross sections by Bass and Paur (1985) are used. A more recent ozone cross section data set has been produced by Serdyuchenko et al. (2011), at Institute of Environmental Physics (IUP), University of Bremen. They have also determined coefficients for second degree polynomials taking ozone temperature as input variable. Ozone cross sections, converted into absorption coefficients (k_o of unit: cm^{-1}), are shown for the UV-PFR#1001 and a general Brewer spectrophotometer in tables 4 and 5, respectively. "B&P" stands for Bass and Paur (1985), "IUP QFT" are results from the Serdyuchenko et al. temperature quadratic fit coefficients and "IUP 5dig" are results linearly interpolated to -45°C from cross sections given at 223 K and 233 K in the data file serdyuchenkogorshlev5digits.dat (available 2016.04.15 at <http://www.iup.uni-bremen.de/gruppen/molspec/databases/referencespectra/o3spectra2011/index.html>). The given ozone absorption coefficients have been calculated by convolving high spectral resolution absorption coefficients with both slit functions/filter functions and extra-terrestrial solar spectrum.

Again, the difference in derived AOD based on different ozone cross section datasets is highly significant at the shortest wavelengths. At the 305.3 nm wavelength of the UV-PFR the difference is as high as >0.022 for a 350 DU ozone amount. Differences at the other wavelengths are given on the last row of table 3. In figure 3 the average reference AOD derived from UV-PFR measurements during the 10th RBCC-E campaign using different versions of absorption coefficients are shown. Clearly, the difference between using Bass and Paur (1985) compared to Serdyuchenko et al. (2011) ozone absorption coefficients is largest at the shortest wavelengths. By using Serdyuchenko et al. (2011) ozone absorption coefficients the resulting AOD actually decreases with decreasing wavelengths for $\lambda \leq 313.5$ nm. This is not expected for most aerosol size distributions, at least not in the UVA-NIR spectral range. Level 1.5 data from the relatively close AERONET station in Huelva had an average value of Ångström's wavelength exponent α (over the wavelength range 440-1020 nm) of 1.14.

The error caused by not using individual wavelengths for each Brewer is bigger for the ozone optical depth than for the Rayleigh optical depth. For a 350 DU TCO value the ozone optical depth error was calculated to <0.005 at 306.3 nm and <0.003 at the other wavelengths for a Brewer with central wavelength(s) deviating by two standard deviations from the mean. Even if the error is relatively small, in the future, in calibrations and AOD analysis performed by the author of this report the individual Brewer wavelengths should be used.

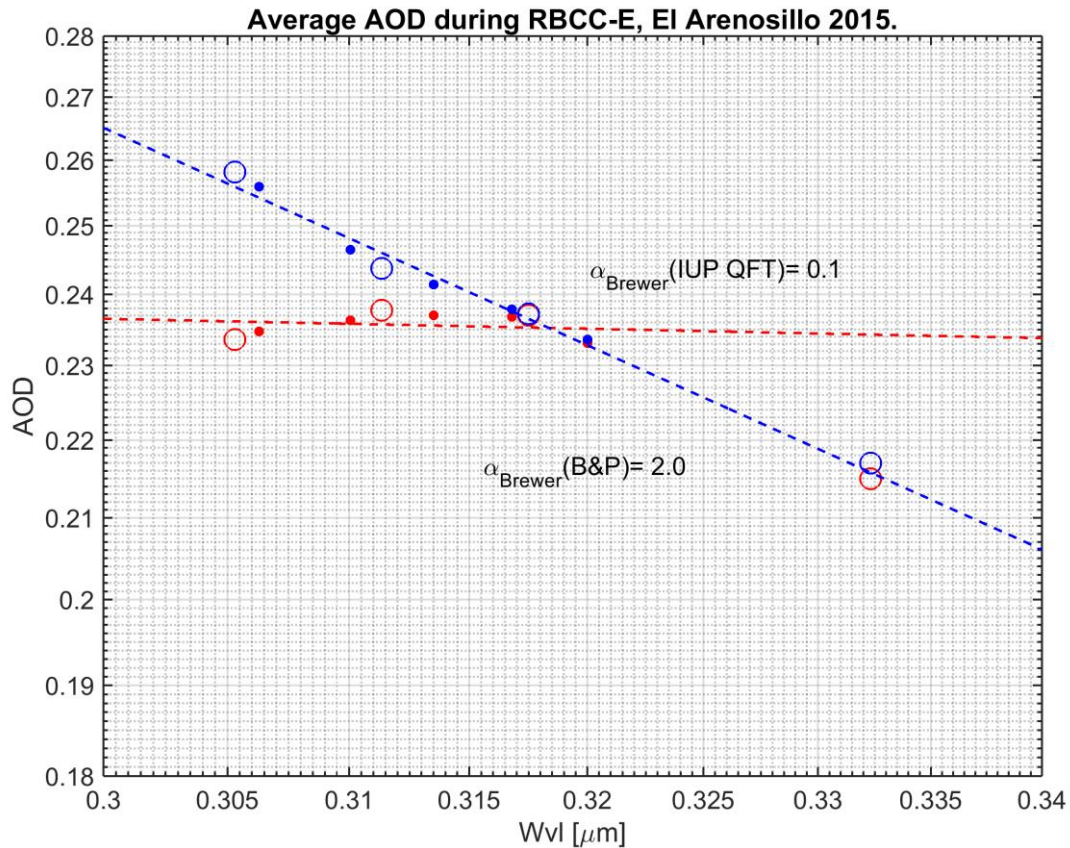


Figure 3. Average aerosol optical depth from the UV-PFR#1001 during the 10th RBCC-E campaign at El Arenosillo 2015. Rings: AOD at UV-PFR wavelengths. Dots: AOD interpolated to Brewer wavelengths. Red: AOD calculated using B&P ozone absorption coefficients. Blue: AOD calculated using IUP QFT ozone absorption coefficients. Ångström's wavelength exponents (α) are calculated from AOD at the Brewer wavelengths only. The ozone amount used in the AOD calculations is the ozone resulting from using correct Rayleigh optical depth coefficients for the Brewer.

It can not be concluded here which set of absorption coefficients that results in AOD values closest to the truth at wavelengths <315 nm. For simplicity and consistency with the ozone determination the first AOD version in the EUBREWNET database could be based on the Bass and Paur (1985) absorption coefficients.

The ozone absorption coefficients are dependent on the temperature distribution through the ozone layer. But since the ozone absorption coefficients are calculated for a constant effective ozone temperature of -45 °C for both the Brewers and the UV-PFR, there will not be an effect on AOD from a temperature difference between the instruments. The effect of using erroneous effective ozone temperature can be significant. Ozone absorption coefficients calculated for -50 °C and -40 °C using the quadratic fit coefficients by Serdyuchenko et al. (2011) result in AOD differences of almost +0.01 and -0.01, respectively, at the 306.3 nm wavelength for TCO=350 DU. This effect/error decreases with wavelength and at 320 nm the effect is instead only about ± 0.002 . The effect/error approximately doubles for ± 10 °C temperature error.

Calibration methods

Calibration of reference instruments

Calibration of reference instruments for AOD determination is normally made at high altitude stations with stable cloud-free atmospheric conditions, low and stable aerosol load and, for instruments measuring at wavelengths affected by absorption in ozone, also stable total ozone amount. These requirements can relatively frequently be fulfilled at the Izaña Atmospheric Observatory (IZO) on the island of Tenerife, at 28°18'N, 16°29'W, 2373 m.a.s.l.

The classic Langley method to determine the calibration constant I_0 (Brewer) or V_0 (UV-PFR) of each channel, being equal to the signal that would have been measured at the top of the atmosphere at mean Sun-Earth distance, has been described in many articles on sunphotometry (e.g. Shaw, 1983) and many variations thereof have been published over the last 30 years. (In the following the spectral irradiance signal will be denoted V as is often the case in sunphotometry.) It is based on the inversion of the so-called Beer-Bouguer-Lambert's law for monochromatic radiation, leading to

$$\ln(V) = \ln(V_0) - \delta m \quad (2)$$

where the wavelength dependent quantities $\ln(V_0)$ and total optical depth δ can be determined by least-square methods from a number of cloud-free measurements of V taken at different air masses m . The calibration constant V_0 used to be found by linear extrapolation of measurements V plotted on a logarithmic scale versus air mass to zero air mass, and this method is historically called Langley plot calibration.

Using a single, common air mass m for all components of the total optical depth can lead to significant errors in $\ln(V_0)$, an example will be given below. A more accurate variant of the Langley extrapolation used here replaces δm by the sum of the individual optical depth components $\delta_R m_R + \delta_o m_o + \delta_a m_a$ (the same terms as in equation 1) and solves the equation

$$\ln(R^2 V) + \delta_R m_R = \ln(V_0) - (\delta_o + \delta_a) m_{2ODW} \quad (3)$$

for $\ln(V_0)$ and the sum of the two terms ozone and aerosol optical depth ($\delta_o + \delta_a$). As above, R is the actual Sun-Earth distance expressed in AU. The air mass term m_{2ODW} is the ozone and aerosol optical depth weighted sum of m_o and m_a . The values on ozone and aerosol optical depth are calculated from total ozone measured by the Brewer triad (Brewers #157, #183 and #185) and from the AOD measured by either PFR-N06 or PFR-N21 and extrapolated to the actual UV wavelength using the Ångström relation. As discussed below this Langley plot method gave the least erroneous results of V_0 due to the effect of finite spectral bandwidth of the UV-PFR filters. This method is therefore used for the calibration of the UV-PFR#1001 as analysed by the PMOD group.

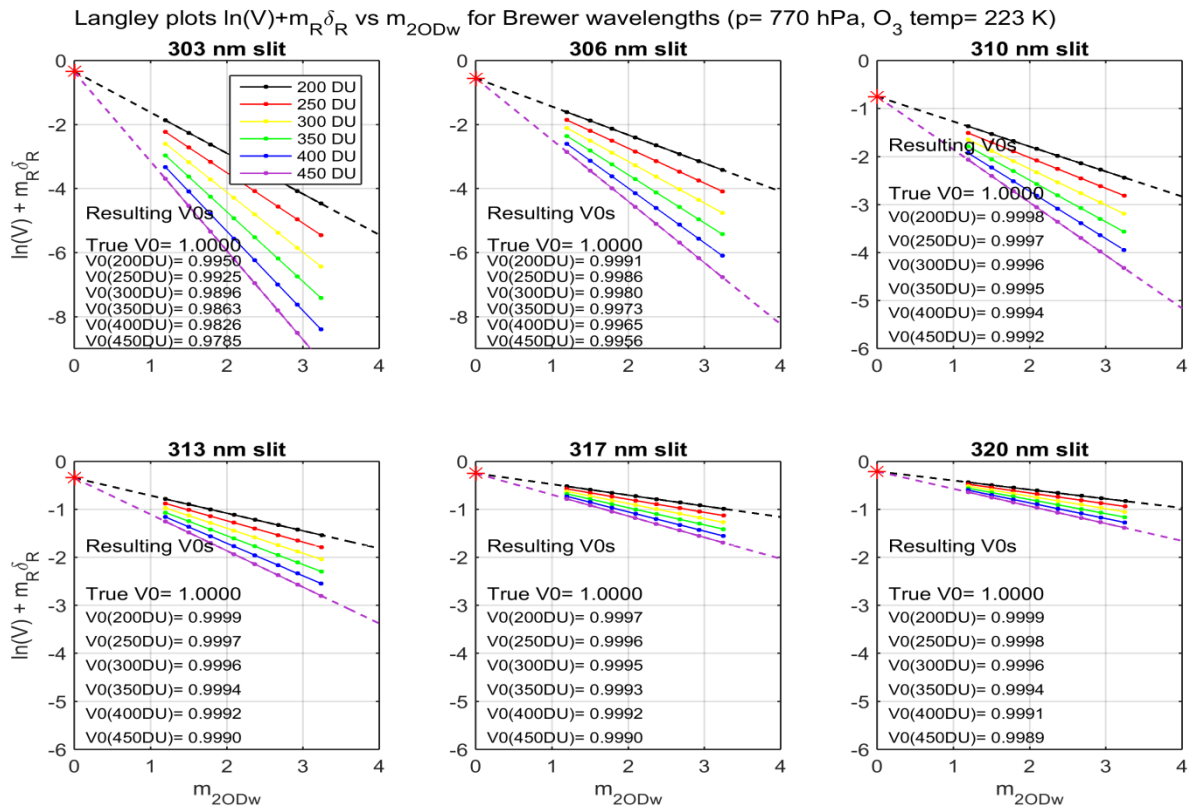


Figure 4. Langley plot modelling results for $\ln(V)+m_R\delta_R$ versus m_{2ODw} for Brewer slit functions.

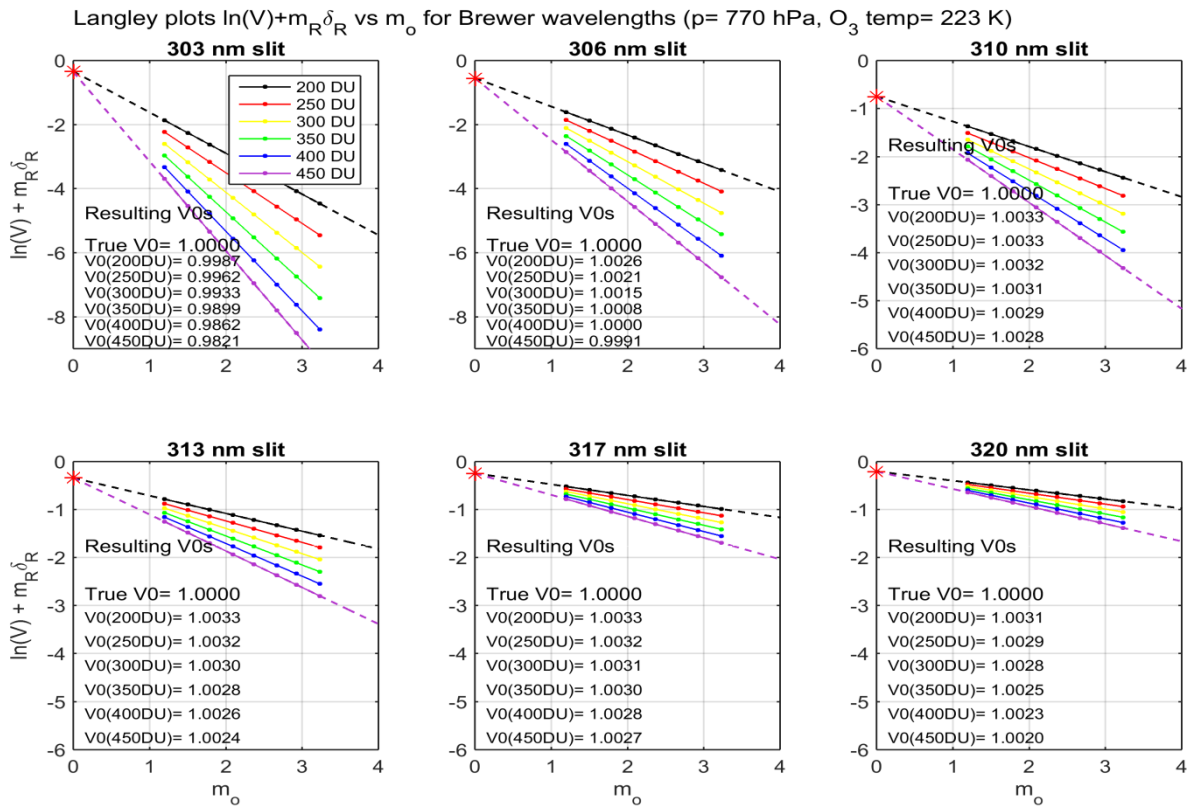


Figure 5. Langley plot modelling results for $\ln(V)+m_R\delta_R$ versus m_o for Brewer slit functions.

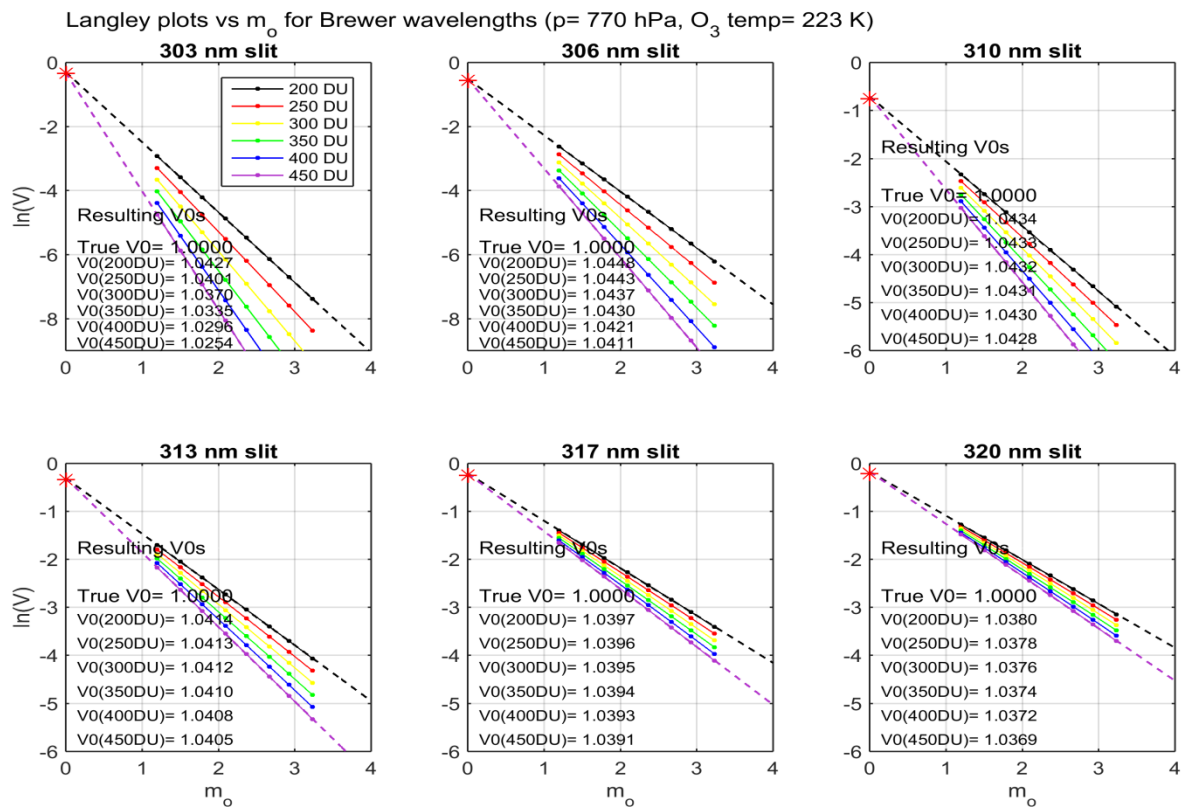


Figure 6. Langley plot modelling results for $\ln(V)$ versus m_o for Brewer slit functions. Here the effect of using an incorrect air mass term is clear.

For Brewer spectrophotometers it is also possible to do the Langley regression using only the relative optical air mass for ozone, m_o , (figure 5) since the ozone optical depth normally is several times higher than the aerosol optical depth at the wavelengths 306.3 – 320.0 nm at the high altitude Izaña Observatory. An advantage is that this method can be used without any other AOD or ozone measurements as input. This method is used for the calibration of Brewer #185 as analysed by the IARC group.

Langley plot method comparison and effect of finite FWHM

For Langley calibrations of spectral solar radiometers the method of the Langley plot as well as the spectral resolution of the measurements affect the calibration result (in addition to small ozone and aerosol variations during real Langley periods). To quantify the influence of method and spectral resolution some simple but high spectral resolution modelling using Beer-Bouguer-Lambert's law was done.

Using an extra-terrestrial solar spectrum of 0.01 nm resolution (Egli, et al. 2012), together with ozone absorption coefficients from Molecular Spectroscopy Lab at IUP Bremen (Serdyuchenko, et al., 2011) interpolated from 0.02 nm to 0.01 nm resolution, and AOD following the Ångström law with the parameters $\alpha=1.3$ and $\beta=AOD_{100nm}=0.012$ (giving $AOD=0.055$ at $\lambda=310$ nm), direct solar irradiance spectra at the surface were calculated for different air masses and total column ozone amounts. In the calculations a station pressure of 770 hPa was used which is close to the average value at the IZO station during the evaluated Langley plot events. Effective ozone altitude and temperature were set to 22 km and -50 °C, respectively. Rayleigh optical depth, $\delta_{R,\lambda}$, was calculated according to Bodhaine, et al. (1999, equation 30) and the relative optical air mass for Rayleigh scattering was calculated according to Kasten and Young (1989). The aerosol relative optical air mass, m_a , was estimated by an

algorithm for water vapour air mass, m_w (Gueymard, 1995). The vertical distribution of the aerosol particles is generally not known but also in other AOD calculations the aerosol air mass have been approximated by estimated m_w , e.g. for the GAW PFR network (McArthur et al., 2003; Wehrli, 2008). Finally, the calculated irradiance spectra were convolved with general 0.55 nm FWHM slit functions (triangular with flat top) for a Brewer spectrophotometer.

Results of Langley plots of the simulated Brewer direct irradiances (here still denoted by V , as often used as irradiance signal in sunphotometry) were then compared to the extra-terrestrial irradiances calculated by convolving the extra-terrestrial spectrum with the Brewer slit functions. In figure 4 it can be seen that for Langley plots of $\ln(V)+m_R\delta_R$ versus m_{2ODW} (for which correct air mass terms are used) of the modelled Brewer irradiances the extra-terrestrial constants are slightly underestimated. The difference between Langley plot V_0 and true V_0 is caused by the finite FWHM of the measurements. For wavelengths ≥ 310 nm the effect of finite FWHM is negligible. At the 306 nm slit the FWHM effect is in the order of only 0.3 % for 350 DU TCO, thanks to the narrow slit function in the Brewer. If Bass and Paur (1985) ozone absorption coefficients are used instead, the estimated FWHM effect becomes 0.5 % at the 306.3 nm wavelength, but remains negligible at longer wavelengths. The underestimation of the calibration value, V_0 , increases with total column ozone amount. The underestimation also increases (decreases) if the air mass range at the high end increases (decreases) (not shown).

In figure 5, the modelled measurement points are fitted against (only) ozone air mass, m_o . For the AOD and aerosol air mass used in this modelling the extrapolated V_0 values are now slightly over-estimated by about 0.3 %. The exception is the 306.3 nm slit where the effect of finite FWHM and slightly erroneous air mass term nearly cancel each other for a TCO amount of 350 DU. This is the Langley plot method used by the IARC group for the Izaña Brewers. Any corrections for the small FWHM effects found here are not applied.

The errors introduced by using the Langley method shown in figure 5, is an order of magnitude less than the errors resulting from the simplified Langley method by fitting $\ln(V)$ versus m_o , shown in figure 6. The Rayleigh optical depth term is not handled separately here, and since the Rayleigh optical depth and the ozone optical depth are of the same order of magnitude (or even $\delta_R > \delta_o$), while their effective vertical distribution differs significantly, significant errors in the extrapolated extra-terrestrial constants (V_0) are introduced.

The same Langley plot modelling has been performed for the UV-PFR. The filter functions of the UV-PFR have FWHMs of 1.0 – 1.3 nm, table 6, which are significantly wider than the Brewer FWHMs. For the shortest wavelength, 305.3 nm, this results in an underestimated V_0 of about 1.4 % for a 300 DU TCO. The average total column ozone amount at IZO during the Langley calibrations in 2015 of the UV-PFR was 292 DU, and the minimum and maximum ozone amounts during any of the Langley periods were 282 DU and 311 DU, respectively. Therefore, the Langley modelling results for the 300 DU ozone amount were taken into account and the mean of V_0 s derived from the accepted Langley plots were multiplied by $C_{FWHM}=[1.014 \ 1.003 \ 1.001 \ 1.000]$ for the UV-PFR channels from the shortest to the longest wavelength. These values are in line with corrections calculated for 2 nm FWHM using a more comprehensive model (Slusser et al., 2000).

Table 6. Wavelength characteristics of UV-PFR#1001 based on laboratory measurements February 2016. The third column show effective central wavelength resulting from convolving the spectral response function with an extra-terrestrial solar spectrum.

Channel (nm)	Effective central wavelength (nm)	Convolved effective central wavelength (nm)	Bandwidth FWHM (nm)
305	305.35	305.31	0.99
311	311.36	311.34	1.04
318	317.55	317.50	1.20
332	332.33	332.32	1.26

With the wider bandwidths of the UV-PFR, not only the derived V_0 s are affected by the FWHM effect due to the rapidly changing ozone absorption with wavelength. Even if the correct V_0 are used, the calculated AOD will still be incorrect if not a further correction is applied. With increasing air mass there is an increase in effective central wavelength for the sunphotometer channels as mentioned above. This results in an apparent decrease in ozone optical thickness with increasing air mass. This effect was quantified by calculating the ozone optical depth from the modelled UV-PFR direct

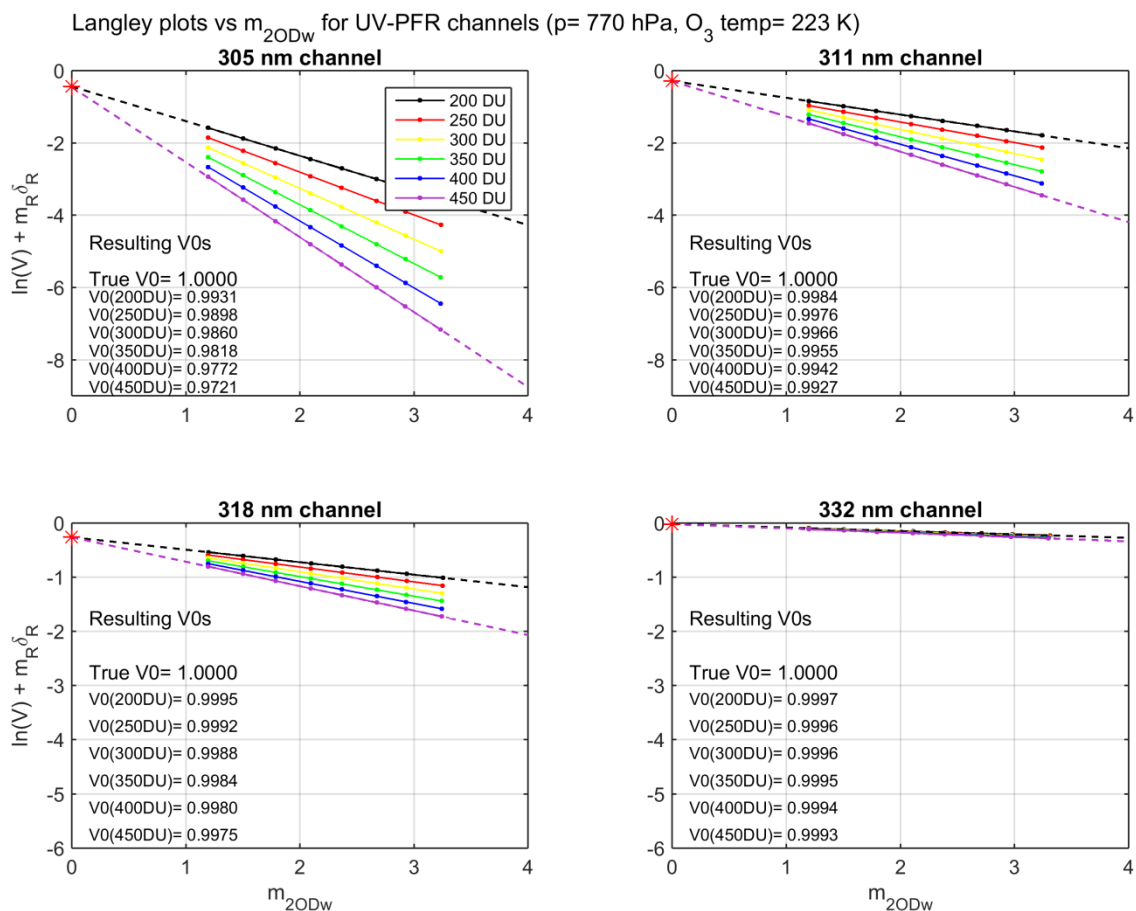


Figure 7. Langley-plots of modelled direct irradiance signals for an UV-PFR sunphotometer. m_{2ODw} is the ozone and aerosol optical depth weighted air mass.

irradiance signals using the Rayleigh and aerosol optical depth values at their fixed effective central wavelengths. The effect varies slightly with station altitude/pressure. Since the UV-PFR so far has been used at Izaña (ca. 2370 m a.s.l.), Davos (ca. 1650 m.a.s.l.) and El Arenosillo (close to sea level) results are shown for approximate pressure level of Davos in figure 7. Again, the “problems” are worst for the shortest wavelengths. The effect is negligible at the 332 nm wavelength.

The apparent change in ozone optical depth is not a perfect linear function with air mass. However, for simplicity, the ozone optical depth correction is here estimated as a linear function of m_o with the lines passing through the origin. The error in the derived AOD using this simplification is according to the calculations performed here ≤ 0.001 units of AOD at the shortest wavelength and high total ozone amount, and considerably smaller at the other wavelengths. The resulting ozone optical depth correction factor for 350 DU total column ozone, $\Delta\delta_{o,350DU}$, is given in table 7. The apparent decrease in ozone optical depth increases with the total column ozone. The ozone optical depth change for 350 DU is taken as reference. Then the ratio of the O_3OD change at other ozone amounts at a specific m_o is very similar for all wavelengths and can be approximated by a quadratic polynomial as

$$f_{o,DU} = \Delta\delta_{o,DU} / \Delta\delta_{o,350DU} = 6.1974e-6 * (TCO)^2 + 0.8359e-3 * TCO - 0.0523 \quad (4)$$

where TCO is the total column ozone amount expressed in Dobson units. All in all, at an air mass of 2 and total column ozone amount of 300 DU the effect of the FWHM corrections on derived AOD at

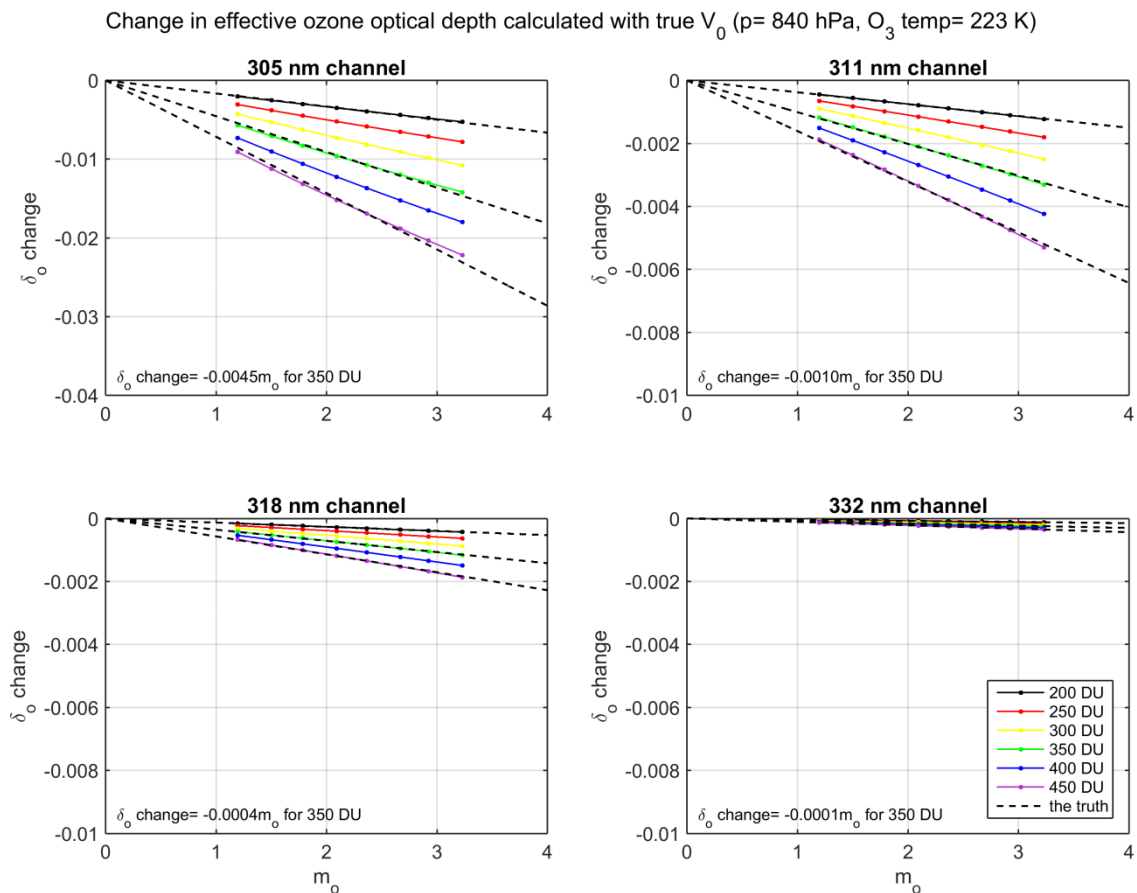


Figure 8. Calculated change in effective ozone optical depth with air mass due to the UV-PFR filter bandwidths.

Table 7. Langley calibration results for UV-PFR#1001 at Izaña 2015, together with calculated V_0 and δ_o FWHM correction factors.

Channel (nm)	L-plot V_0 (mV)	Std. dev. of L-plot V_0 (%)	FWHM correction factor for V_0	δ_o correction factor for 350 DU, $\Delta\delta_{o,350}$
305	30338	1.1	1.014	-0.0045
311	11539	0.6	1.003	-0.0010
318	10673	0.8	1.001	-0.0004
332	5308	0.4	1.000	0

305 nm is about +0.016, while it is only about +0.004 at 311 nm. Both these values are much lower than the total uncertainty in the UV AOD but since the errors due to the finite FWHM are systematic the relatively small corrections are still performed. As good measurement practice, all known biases should be removed or corrected (GUM, 1995).

Finally, from the Beer-Bouguer-Lambert law, and including the FWHM corrections described above, the spectral aerosol optical depth at wavelength λ is for the UV-PFR calculated as

$$AOD_\lambda = \delta_{a,\lambda} = \ln\left(\frac{C_{FWHM}V_{0,\lambda}}{R^2V_\lambda}\right)/m_a - \frac{m_R p}{m_a p_0} \delta_{R,\lambda} - \frac{m_o}{m_a} (\delta_{o,\lambda} + f_{o,DU} \Delta\delta_{o,\lambda,350DU} m_o) \quad (5)$$

from the measurements of the spectral UV-PFR output signals V_λ . The $V_{0,\lambda}$ are the calibration constants derived from Langley plot calibrations of the UV-PFR#1001 at the high altitude station IZO as described above.

Effect of internal polarization in the Brewers

For the Brewer spectrophotometers, there is another important effect to take into account in the Langley plot calibrations, namely the effect of internal polarization which occurs at the flat entrance window and at the internal grating. In an article by Cede et al. (2006) the effect of internal polarization in Brewer MkIII was studied. They presented both theoretical and experimental results of the effect. They recommended the experimental results to be used.

Based mainly on the theoretical results of Cede et al. (2004, 2006) for MkIII Brewers a Matlab function for polarization correction has been developed by Henri Diémoz (personal communication 2015). The validity of the theoretical results for MkIII Brewers was investigated during the 10th RBCC-E campaign (Diémoz and Carreño, personal communication, 2015) and tested also for other Brewer models. For MkII and MkIV Brewers a percentage of light transmitted in the vertical polarization must be also accounted for.

The experimental (AC) and theoretical (HD) polarization effect are shown in figure 8 which displays the ratio of instrument sensitivity at various zenith angles to the sensitivity at normal incidence (solar zenith angle, SZA= 35°). The experimental results of Cede et al. 2006 were only determined for SZA≥55° (crosses and red dots in figure 8). The theoretical estimate gives a stronger polarization

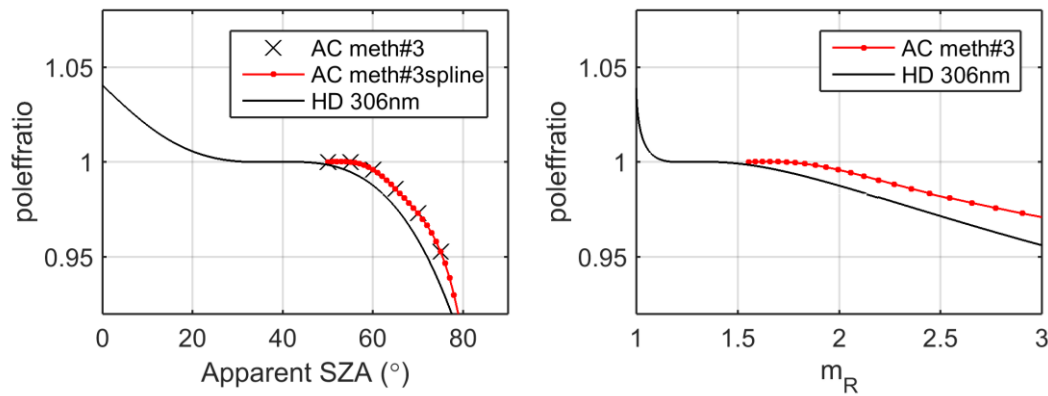


Figure 9. Effect of internal polarization for a Brewer MkIII. AC is polarization effect determined experimentally and recommended by Cede et al. (2006), HD is theoretical polarization effect for the 306 nm wavelength, coded into a Matlab-function by Henri Diemoz (ARPA, Italy).

effect than the experimental estimates by Cede et al. (2006). The influence of internal polarization on Langley plot results is large, in the order of 2-4 %, and increases with increasing air mass range on the high end. Calibration results from both versions of polarization corrections will be investigated in the following. (OR: Based on the recommendations of Cede et al. (2006) and the results of calibrations of Brewer #185 versus UV-PFR reference AOD and Langley plots at Izaña shown below, the experimental polarization correction by Cede et al. at SZA $\geq 55^\circ$ will be used for the Brewer Langley calibrations in the following.)

Langley selection criteria

Of importance for the final calibration constants to be used is of course also how accepted Langley plot events are selected. The approach for the UV-PFR Langley calibration (by the author of this report) was to use information from accurate measurements of TCO and AOD in the UV-NIR spectral range, which indeed can be available from the Izaña observatory. Based on these additional measurements, clear sky periods with both stable ozone amount and AOD were simply found/chosen by manual inspection of the ozone and AOD data during potential Langley periods. For the identified Langley periods the linear change of TCO with air mass was calculated ($\Delta DU/\text{unit air mass}$). The calculated $\Delta DU/\text{unit air mass}$ can then be used to either interpolate the final V_0 for zero ozone change, or the mean of individual V_0 for which the $\Delta DU/\text{unit air mass}$ was within $\pm 1 \text{ DU}/(\text{unit air mass})$, see figure 9. Again, it is the shortest wavelength that have significant, not to say large, dependence on even small ozone changes during the Langley periods.

The drawbacks of this method is of course the need for the additional high quality data, which can take a considerable time to produce, due to the careful calibration that first has to be done of the ozone (Brewer) and AOD (PFR) measurements. The results will also be dependent on the calibration of the accompanying measurements. In case there is a false air mass dependence in the ozone and/or UVA-VIS AOD measurements, the resulting V_0 for the UV-PFR will also be wrong. Currently, this risk is considered worth to take since both the Brewer triad as well as the reference PFRs at Izaña are thought to be among the most accurate measurements in Europe. To some degree, this method also has some human influence in the semi-manual selection process and therefore it will not be totally objective.

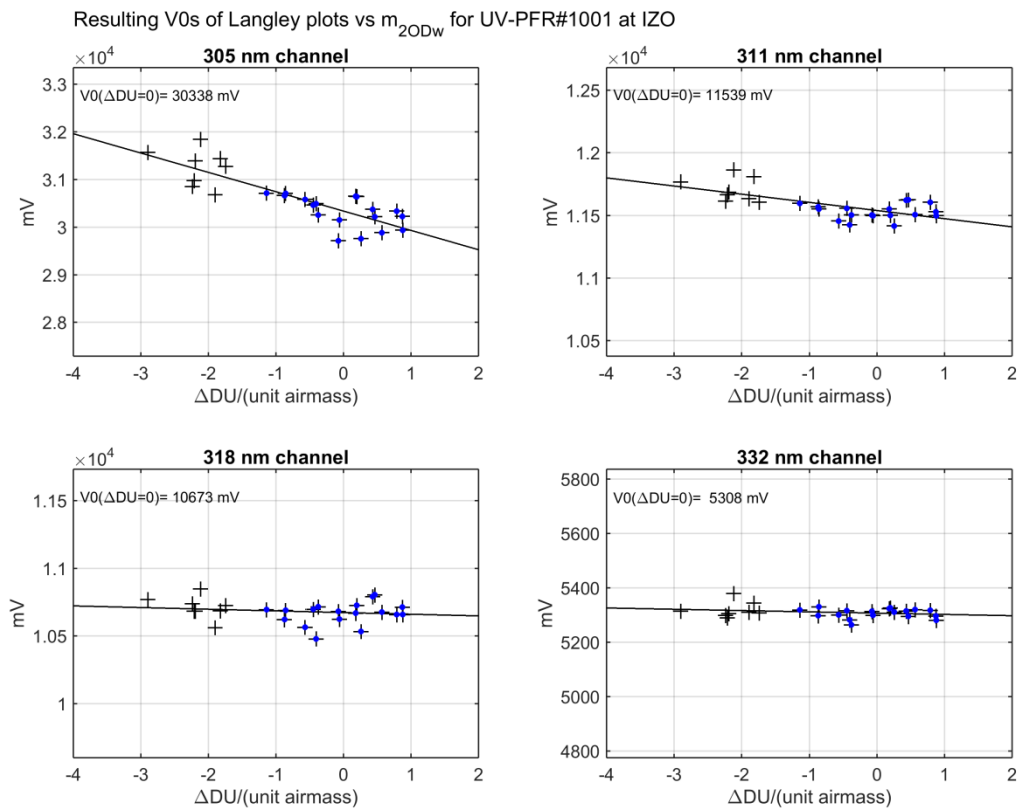


Figure 10. Results of all the Langley plot calibrations of UV-PFR#1001 at IZO during May-August 2015. The points when the change in total ozone during the Langley period was $< \pm 2$ DU are marked with blue dots. The final V_0 s are derived from linear interpolation at zero ozone change. The ozone change during each Langley episode is calculated from linear fit of the Brewer triad total ozone values versus ozone air mass during the Langley plot period.

On the contrary, for the absolute calibration of the Brewers for AOD determination done by the IARC group, the Langley calibration selection criteria are fully based on objective routines. Langley fits are also made individually for each neutral density filter in use. Only Langley periods for which r^2 coefficients of determination are > 0.9985 are considered. Among the calibration values determined with this first criterion fulfilled only those points that are within $\pm 20\%$ of the mean are included in the calculation of the final mean I_0 s.

One might risk getting a higher standard deviation of the I_0 values with this method, since no restriction on ozone change is taken into account. Also, an average ozone or aerosol change with air mass might not be discovered. Large ozone changes will mostly not result in r^2 value of > 0.9985 . For the remaining Langley events it is assumed that the ozone and AOD changes are randomly distributed around zero. Nevertheless, the objectivity of the method and the possibility to make the Langley calibrations without any dependence on additional measurements are of course big advantages of this Langley selection method.

Calibration of field instruments

At the 10th RBCC-E campaign at the El Arenosillo station both the Brewer #185 and the UV-PFR#1001 can provide calibrations of the participating “field” Brewers. Calibration constants for AOD determination, $I_{0,\lambda}$, for the field Brewers were calculated as

$$I_{0,\lambda} = R^2 I_{\lambda} \exp(\delta_{R,\lambda} m_R + \delta_{o,\lambda} m_o + \delta_{a,\lambda,ref} m_a) \quad (6)$$

with $\delta_{a,\lambda,ref}$ derived from Brewer #185 (IARC analyses) or from UV-PFR#1001 (PMOD analyses). While the Brewer measurements were made simultaneous using common measurement schedules, the $\delta_{a,\lambda,ref}$ from the UV-PFR needed to be interpolated to the Brewer ds measurement times and wavelengths. I_{λ} are the ds measurement signals from the Brewer given in photons/s at the respective wavelengths. The other parameters of equation 8 were calculated using the same algorithms as were used for the Brewer and UV-PFR measurements, respectively (table 1). The UV-PFR and the Brewers differ largely in wavelengths. As mentioned earlier, for the calibration of the Brewers against the UV-PFR, calculations were made for the same general wavelengths for all Brewers. The reference AOD values from the UV-PFR were interpolated from the two closest wavelengths on each side of a Brewer wavelength using the Ångström power law. The IARC calibration of the Brewers against Brewer #185, were made using the unique wavelengths determined for each Brewer. Consequently, also unique values on δ_R and δ_o were used.

Comparison of calibration results for Brewer #185

Brewer #185 have been used to compare the calibration results (I_0) derived by the groups at IARC and PMOD. Langley calibrations of Brewer #185 has been performed independently by the IARC and PMOD groups. The IARC results were supplied by Javier Lopez Solano (JLS) and the PMOD results were derived by the author of this report (TC). In TC’s analysis, only measurements taken during 8th of May – 10th of June were analysed for Brewer #185 at Izaña. At the time for this analysis final ozone data from the Brewer triad at Izaña was only available from May 2015 and onwards. As described above, the reference ozone data was simply used to find Langley periods with only small changes in total ozone. After 10th of June, there were instrument changes of Brewer #185 resulting in incomparable Langley plot results at later dates. Since Brewer #185 was participating in the RBCC-E campaign end of May - early June, only 5 accepted Langley plot events were found for TC’s Langley plot calibrations. Of course, this leads to rather high uncertainty in TC’s average Langley plot I_{0s} . In JLS’ analysis 24 valid Langley periods were found during April and May 2015 at Izaña.

For the AOD calibrations at the RBCC-E campaign versus UV-PFR#1001 individual I_0 are determined for each ND filter in use. Also the Langley calibrations at Izaña done by IARC are made individually for each ND filter. This is normally not the case for the Langley calibration done by TC. At the RBCC-E campaign, the majority of the AOD calibration points for Brewer #185 were taken using ND#3. Therefore, for this comparison, the Langley calibrations performed by TC were limited to the air mass range of approximately 1.2-2.3, when only measurements with ND#3 were used. This air mass range is very small, but in addition to using measurements from only one ND filter, the effect of internal polarization is also reduced compared to the case when also measurements at higher air masses are included.

As a final restriction, for the calibration of Brewer #185 at El Arenosillo (ELA) only the days which were judged as good and undisturbed measurement days have been considered. Brewer#185 was

Table 8. Calibration results for Brewer #185 based on calibration versus UV-PFR#1001 at El Arenosillo (ELA) and based on Langley-plots at Izaña Observatory (IZO) by IARC/JLS and PMOD/TC independently. For the calibrations at ELA, zone absorption coefficients by Bass and Paur (1985) were used. I_0 in units of 10^6 photons/s.

Result No.	Resulting I_0 s for Brewer #185 from ELA (vs UV-PFR#1001) and from Langley plots at IZO										
	Calibration site, ND, etc.	I_0 306.30	stddev (%)	I_0 310.05	stddev (%)	I_0 313.50	stddev (%)	I_0 316.80	stddev (%)	I_0 320.00	stddev (%)
#1	ELA, good days, ND#3 only, with polariz. corr. by HD	115.06	0.4	91.31	0.5	149.61	0.5	153.17	0.5	165.71	0.4
#2	ELA, good days, ND#3 only, without polariz. corr.	115.43	0.5	91.59	0.5	150.1	0.5	153.67	0.5	166.22	0.5
#3	IZO(TC), L-plot, ND#3 only, with polariz. corr. by HD	111.99	1.3	88.97	0.9	146.36	0.9	149.02	0.8	162.13	0.8
#4	IZO(TC), L-plot, ND#3 only, with polariz. corr. by AC	114.43	1.1	90.61	0.6	149.16	0.7	151.78	0.6	165.27	0.7
#5	IZO(TC), L-plot, ND#3 only, without polariz. corr.	115.55	1.2	91.79	0.5	150.98	0.6	153.71	0.5	167.23	0.6
#6	IZO(JLS), L-plot, ND#3 only, with polariz. corr. by AC	114.83		90.14		148.08		150.39		164.34	
#7	IZO(JLS), L-plot, ND#3 only, without polariz. corr.	117.36		91.94		150.90		153.12		167.30	
	Some ratios										
	With/Without polariz. corr. ND#3 at ELA, #1/#2	0.997		0.997		0.997		0.997		0.997	
	ELA/IZO(TC), ND#3 only, with polariz. corr. by HD, #1/#3	1.027		1.026		1.022		1.028		1.022	
	ELA/IZO(TC), ND#3 only, with polariz. corr. by HD/AC, #1/#4	1.006		1.008		1.003		1.009		1.003	
	IZO(TC)/IZO(JLS), ND#3, with polariz. corr. By AC #4/#6	0.997		1.005		1.007		1.009		1.006	
	IZO(TC)/IZO(JLS), ND#3, without polariz. corr. #5/#7	0.985		0.998		1.001		1.004		1.000	
	ELA/IZO(JLS), ND#3 only, with polariz. corr. by HD/AC, #1/#6	1.006		1.008		1.003		1.009		1.003	

one of those instruments that suffered from the apparent decrease in sensitivity during the days 150-152 which may have been caused by accumulation of dust on the window (Carlund et al., 2016, in preparation).

For the calibration results versus UV-PFR#1001 at the ELA campaign, the ozone absorption coefficients by Bass & Paur (1985) were used in the calculations of the reference AOD values.

The I_0 results of Brewer #185 (good days) versus the UV-PFR#1001 during the RBCC-E campaign at El Arenosillo (ELA) and from Langley-plots at Izaña are listed in the upper part of table 8. Also the standard deviations of the I_0 :s are shown for the ELA calibration and the IZO Langley calibration by TC.

In the lower part of table 8 ratios between different calibration results are given. From the calibration results it is clear that Langley plot results from IZO derived without any polarization correction resulted in the highest extra-terrestrial constants I_0 . The two Langley results without polarization correction (results #5 and #7) are however very close to each other. For the two Langley results using the same polarization correction (results #4 and #6), the results are within ± 1 % of each other at all wavelengths. Even though the agreement is not perfect, and that only 5 Langley events

were used in TC's analysis, the results indicate that Langley analyses are consistently made by the two groups.

By applying the theoretical polarization correction, i.e. the HD polarization correction function, the Langley plot calibration by TC decreases the I_0 values by as much as 3 % (result #3), even for the small air mass range considered here, compared to the results without any polarization correction (result #5). The I_0 values of Brewer#185 from ELA are in this case 2-3 % higher than the Langley plot results (table8, ratio #1/#3).

The experimentally determined polarization effect by Cede et al. (2006) indicated that the true internal polarization effect is actually somewhat weaker than what is estimated by the theoretical calculations (crosses and red curves in figure 9). For polarization correction of Brewer MkIII direct irradiance measurements Cede et al. (2006) recommended that the experimental results are to be used. Using these results to correct the Brewer#185 in Langley plot calibrations results in extrapolated I_0 values that at all wavelengths are within ± 1 % of the calibration results from the RBCC-E campaign (table 8, ratios #1/#4 and #1/#6). The experimentally measured polarization effect by Cede et al. only covered solar zenith angles $\geq 50^\circ$. Since the theoretical polarization correction gave slightly improved results at the low air mass end this method could be used at the low air mass range, for solar zenith angles $< 30^\circ$, while the experimental polarization correction by Cede should be used for $SZA > 55^\circ$.

The Langley plot results are not dependent on any specific set of ozone absorption coefficients. On the contrary, calibration results versus the UV-PFR based on ozone absorption coefficients by Serdyuchenko, et al. (2011) differs by [-1.3 -0.3 -0.1 -0.2 +0.3] % from the results in table 7, #1, for which Bass and Paur (1985) ozone absorption coefficients were used. The results based on the Serdyuchenko coefficients are still within 1 % from the Langley plot results by TC (#4), but deviates more than 1 % from the results by JLS (#6) at three wavelengths.

From this comparison of calibration results of Brewer #185 it is concluded that the IARC and PMOD produce consistent results for their respective AOD reference instruments, Brewer #185 and UV-PFR#1001, respectively.

Comparison of resulting AOD

As a final comparison, AOD was calculated from measurement data during the RBCC-E campaign at El Arenosillo 2015 using the calibration results from the IARC and PMOD groups respectively. The results for Brewer #163 are plotted in figure 11. In the AOD calculations, both groups used Rayleigh coefficients derived according to Bodhaine et al. (1999), ozone absorption coefficients according to Bass and Paur (1985). The ozone amount was also corrected for the erroneous default Rayleigh coefficients in the Brewer ozone retrieval. For $SZA > 50$ the experimental polarization correction by Cede et al. (2006) was applied by both groups. Also the same temperature coefficients (applied to ozone measurements) were applied.

Overall the agreement in AOD derived by the two groups is good. In addition to the slightly different calibration results the AOD values at very low m_o differs also due to the fact that the theoretical polarization correction was applied at low solar zenith angles ($< 30^\circ$) in the AOD calculations by PMOD/TC. At the three longest wavelengths, and at air masses > 1.15 , more than 95 % of the data points are within the WMO traceability limits for AOD derived from direct sun measurements made with finite/small field of view instruments (WMO/GAW, 2005).

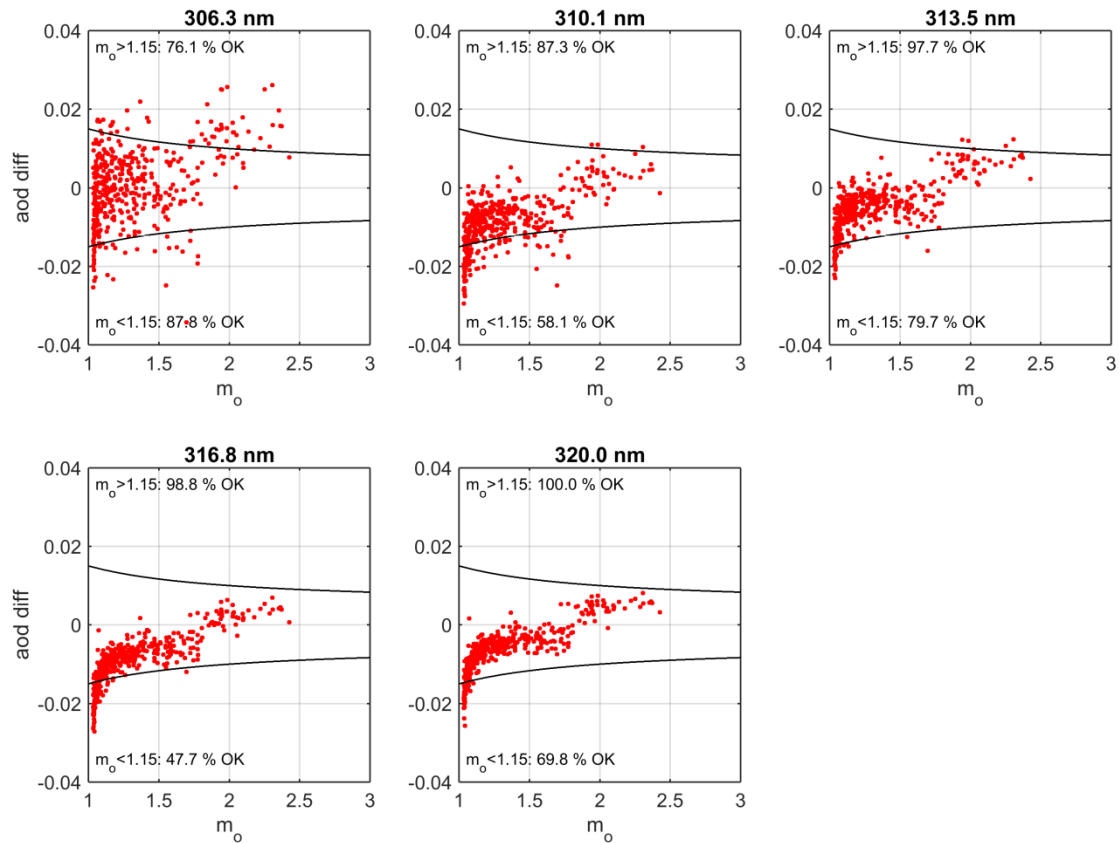


Figure 11. Difference in AOD for Brewer #163 resulting from calibration and AOD calculation by the two groups, IARC-PMOD.

Conclusions

During this short term scientific mission, current calibration methods and algorithms for input variables to AOD retrievals used for Brewer spectrophotometers and UV-PFR sunphotometers, respectively, have been reviewed. The influence of identified differences on resulting AOD has been quantified.

Starting with solar position algorithms and the following air mass calculations only small differences were found. The Brewer algorithm for m_R results in some AOD difference at higher air masses compared to the common equation by Kasten and Young (1989) considered more accurate, which is also used by e.g. the AERONET and GAW/PFR networks.

For the ozone air mass small differences in AOD are introduced when different effective ozone altitudes are used. In the Brewers a constant value of 22 km is used while for the UV-PFR effective ozone altitude is calculated from the ML-climatology (McPeters and Labow, 2012) which is dependent on date and latitude (figure 1). For ozone determination with Dobson spectrophotometers ozone altitude is only latitude dependent (table 2). The effect of different ozone altitude is negligible at the longest Brewer wavelength (320 nm) but it has some influence at the shortest wavelengths at air masses >2 when the effective ozone altitude differs from the used value. For simplicity the constant value of 22 km could be used in the first version of the EUBREWNET AOD

data product. When there is agreement on better ozone altitude values to be used, the AOD product can be updated accordingly.

The default Rayleigh optical depths used in the Brewers results in about 0.008 lower AOD than when more accurate coefficients are calculated using e.g. the algorithm by Bodhaine et al. (1999). Together with the default air mass formula used in Brewers the underestimation of AOD can exceed 0.01. It is strongly recommended that Rayleigh optical depths for the Brewers are updated to values calculated using the Bodhaine et al. (1999) algorithm. To get in better agreement with other (global) AOD networks it is also recommended that the Rayleigh air mass calculations are updated to the algorithm by Kasten & Young (1989). It is important that also the best possible Rayleigh coefficients are used in the ozone determinations.

The difference (and error source) having the potentially largest impact on AOD, in the order of 0.02 at all wavelengths for a pressure error of 20 hPa, is the fact that actual air pressure at the measurement site is not taken into account in the AOD calculations for the Brewers. To improve the AOD data it should be investigated if pressure measurement data could also be submitted from the EUBREWNET sites.

The choice of ozone cross section data set is of great importance of the derived AOD values, especially at the shortest wavelengths for which the ozone absorption is the largest. It can not be concluded here which of the two tested cross section data sets, Bass and Paur (1985) and Serdyuchenko et al. (2011), that is the most accurate at all wavelengths. However, using ozone absorption coefficients by Serdyuchenko et al. resulted in an unexpected decrease of average AOD with decreasing wavelength at $\lambda < 315$ nm, during the 10th RBCC-E campaign. Also the calibration results of Brewer #185 versus the UV-PFR#1001 using the Bass and Paur (1985) ozone absorption coefficients were slightly closer to the Langley calibration results of Brewer #185 (which are independent of ozone cross sections). For these reasons, as well as for simplicity, it is recommended that the Bass and Paur cross sections already in use for the Brewer ozone measurements, also are used for the AOD retrievals.

In the current calibrations and AOD retrievals done by the author of this report, the same general wavelengths are used for all Brewers. In the future, also in calibrations against the UV-PFR the individual wavelengths for each Brewer should be used.

It was shown that for Langley plot calibration of reference instruments, the Langley method must be selected carefully and correct air mass terms must be used for the various extinction terms. It was also shown that thanks to the narrow slit functions in the Brewers, any corrections of the resulting extra-terrestrial constants/calibration constants from the Langley plot don't need to be applied. On the contrary, for the UV-PFR such a correction is needed, due to the wider spectral response functions of this instrument.

Internal polarization effects in the Brewer spectrophotometers affect both the irradiance measurements and the derived AOD and, not least, the calibration of reference instruments with the Langley plot method. The actual polarization effect is not known accurately for every Brewer but the main polarizing elements, the flat entrance window and the internal grating, are the same in all Brewers. The polarizing effect was studied by Cede et al. (2004, 2006) both theoretically and experimentally. In Cede et al. (2006) they recommend that the experimental results should be used for correcting direct irradiance measurements with a Brewer. This is also the method that resulted in

Langley plot calibration results for Brewer #185 being closest to the calibration results of the same Brewer versus the UV-PFR#1001 during the 10th RBCC-E campaign at El Arenosillo 2015. The theoretical polarization correction seem to be too strong, at least at larger solar zenith angles (>50°). Also at the low air mass end, the theoretical polarization correction might be a bit too strong. But based on slightly decreased standard deviation of calibration results for Brewers versus the UV-PFR#1001 and by visual inspection the plotted results the theoretical polarization correction give slightly improved values at low solar zenith angles for many brewers at the RBCC-E campaign (Carlund et al., 2016, in preparation).

What was not specifically investigated in this STSM was the temperature sensitivity of the irradiance measurements with the Brewers. Temperature coefficients are applied to the ozone measurements but the use of these coefficients does not necessarily remove the temperature dependence of the irradiance measurements, they just give the same temperature dependence for all wavelengths. How to determine temperature corrections for AOD retrievals needs to be further investigated.

Brewer #185 was used to compare calibration results derived by the IARC and PMOD groups. To avoid the effect of possibly inconsistent optical density values for the ND filters used, the comparison was limited to measurements with ND filter #3. It was shown that Langley calibration results of this Brewer at Izaña derived by IARC and PMOD agreed well with each other, within ± 1 %, both with and without the experimental polarization correction by Cede et al. (2006). Also the calibration results of Brewer #185 versus the UV-PFR#1001 during the RBCC-E campaign were within ± 1 % of the Langley calibration results using the experimental polarization correction by Cede et al. (2016).

Finally, using the calibration results derived by each group, based on calibration versus Brewer #185 and UV-PFR#1001 respectively, and partly harmonized ways to calculate AOD, it was shown that for a “field” Brewer participating in the 10th RBCC-E campaign the resulting differences in AOD for more than 95 % of the cases were within the WMO traceability limits at $m > 1.15$ for the wavelengths 313.5 – 320.0 nm. At lower air masses, polarization correction is currently treated differently which results in larger differences. How to correct the Brewer direct irradiance measurements for polarization (in the EUBREWNET database and its AOD product) need further investigation.

Acknowledgements

The results derived during this STSM would not have been achieved without the valuable input from and discussions with Javier Lopez Solano and Alberto Redondas, AEMET/IARC, who are gratefully acknowledged for hosting me at AEMET/IARC in Santa Cruz.

References

- Bais, A. F., 1997: Absolute spectral measurements of direct solar ultraviolet irradiance with a Brewer spectrophotometer. *Appl. Opt.*, 36, 5199–5204.
- Bass, A. M. and R. J. Paur, 1985. The ultraviolet cross-sections of ozone. I. The measurements, II – Results and temperature dependence, in: *Atmospheric ozone; Proceedings of the Quadrennial ozone symposium* (edited by C.S. Zerefos and A. Ghazi), 1, 606–616.
- Bodhaine, B.A., N.B. Wood, E.G. Dutton and J.R. Slusser, 1999. On Rayleigh optical depth calculations, *Journal of Atmospheric and Oceanic Technology*, Vol. 16, No. 11 Part 2, pp 1854-1861.

Carlund, T., N. Kouremeti and J. Gröbner, 2016. AOD calibration of Brewer spectrophotometers versus the travelling reference UV-PFR#1001 at the 10th RBCC-E campaign held at INTA, El Arenosillo, Spain, 27. May – 5. June 2015. In preparation.

Cede, A., G. Labow, M. Kowalewski, and J. Herman, 2004. The effect of polarization sensitivity of Brewer spectrometers on direct Sun measurements, in *Ultraviolet Ground- and Space-Based Measurements, Models, and Effects IV*, 5 –6 August 2004, Denver, USA, edited by J. R. Slusser et al., Proc. SPIE Int. Soc. Opt. Eng., 5545, 131– 137.

Cede, A., S. Kazadzis, M. Kowalewski, A. Bais, N. Kouremeti, M. Blumthaler, J. Herman: 2006, Correction of direct irradiance measurements of Brewer spectrophotometers due to the effect of internal polarization, *Geophysical Research Letters*, 33, L02806, doi:10.1029/2005GL024860.

Cheymol, A., and H. De Backer, 2003: Retrieval of the aerosol optical depth in the UV-B at Uccle from Brewer ozone measurements over a long time period 1984-2002. *J. Geophys. Res.*, 108, 4800, doi:10.1029/2003JD003758.

Cheymol, A., H. De Backer, W. Josefsson, and R. Stübi, 2006: Comparison and validation of the aerosol optical depth obtained with the Langley plot method in the UV-B from Brewer Ozone Spectrophotometer measurements. *J. Geophys. Res.*, 111, D16202, doi:10.1029/2006JD007131.

Egli, L., J. Gröbner and A. Shapiro 2012. Development of a new high resolution extraterrestrial solar spectrum. PMOD/WRC Annual report 2012.

Gröbner, J., and C. Meleti, 2004: Aerosol optical depth in the UVB and visible wavelength range from Brewer spectrophotometer direct irradiance measurements: 1991-2002. *J. Geophys. Res.*, 109, D09202, doi:10.1029/2003JD004409.

Gueymard, C., 1995. SMARTS2, a Simple Model for the Atmospheric Radiative Transfer of Sunshine: Algorithms and performance assessment. Tech. Rep. FSEC-PF-270-95, 78m pp. [Available from Florida Solar Energy Center, 1679 Clearlake Rd., Cocoa, FL 32922-5703.]

GUM, 1995. Guide to the expression of uncertainty in measurement, International Organization for Standardization, ISBN 92-67-10188-9.

Kasten, F. and A.T. Young, 1989. Revised optical airmass tables and approximation formula, *Applied Optics* 28, 4735-4738.

Kazadzis, S., A. Bais, V. Amiridis, D. Balis, C. Meleti, N. Kouremeti, C. S. Zerefos, S. Rapsomanikis, M. Petrakakis, A. Kelesis, P. Tzoumaka, and K. Kelektoglou, 2007: Nine years of UV aerosol optical depth measurements at Thessaloniki, Greece. *Atmos. Chem. Phys.*, 7, 2091–2101.

Komhyr, W.D., R.D. Grass, and R.K. Leonard, 1989. Dobson spectrophotometer 83: A standard for total ozone measurements, 1962-1987. *Journal of geophysical research*, Vol. 94, No. D7, 9847-9861.

Kumharn, W., J. S. Rimmer, Andrew R. D. Smedley, T. Y. Ying, and A. R. Webb, 2012: Aerosol Optical Depth and the Global Brewer Network: A Study Using U.K.- and Malaysia-Based

Brewer Spectrophotometers. *J. Atmos. Oceanic Technol.*, 29, 857–866. doi:
<http://dx.doi.org/10.1175/JTECH-D-11-00029.1>

Marenco, F., Di Sarra, A., and De Luisi, J., 2002: Methodology for determining aerosol optical depth from Brewer 300–320 nm ozone measurements, *Appl. Opt.*, 41, 1805–1814.

McArthur, L.J. B., D.H. Halliwell, O.J. Niebergall, N.T. O’Neill, J.R. Slusser, C. Wehrli, 2003: Field comparison of network sunphotometers, in *Journal of Geophysical Research*, Vol. 108, No. D19, 4596.

McPeters, R.D. and G.J. Labow, 2012. Climatology 2011: An MLS and sonde derived ozone climatology for satellite retrieval algorithms, *Journal of geophysical research*, Vol. 117, D10303, doi:10.1029/2011JD017006.

Michalsky, J. J., 1988. The Astronomical Almanac’s algorithm for approximate solar position (1950-2050), *Solar Energy*, Vol. 40, No. 3, pp. 227-235.

Reda, I.; Andreas, A., 2003. Solar Position Algorithm for Solar Radiation Applications. 55 pp.; NREL Report No. TP-560-34302, Revised January 2008.

Redondas, A., R. Evans, R. Stuebi, U. Köhler, and M. Weber, 2014. Evaluation of the use of five laboratory-determined ozone absorption cross sections in Brewer and Dobson retrieval algorithms, *Atmos. Chem. Phys.*, 14, 1635-1648, doi:10.5194/acp-14-1635-2014.

Serdyuchenko, A., V. Gorshlev, M. Weber and J.P. Burrows 2011. New broadband high-resolution ozone absorption cross-sections, *Spectroscopy of Europe*, vol. 23, 6, 2011, pp.14-17.

Shaw, G.E., 1983. Sun photometry, *Bulletin of the American meteorological society*, Vol 64, 4-10.

Slusser, J., J. Gibson, D. Bigelow, D. Kolinski, P. Disterhoft, K Lantz and A. Beaubien, 2000. Langley method of calibrating UV filter radiometers. *Journal of geophysical research* , Vol. 105, No. D4, 4841-4849.

Wehrli, C.J., 2008. Remote sensing of Aerosol Optical Depth in a Global surface network, Diss. ETH No. 17591, (available at <http://e-collection.library.ethz.ch/view/eth:30693>).

WMO, 2009. Operations handbook - Ozone observations with a Dobson spectrophotometer Revised 2008, GAW Report No. 183, WMO/TD No. 1469. Available at https://googledrive.com/host/0BwdvoC9AeWjUazhkNTdXRXUzOEU/wmo-td_1469.pdf (2016-04-21).

WMO/GAW, 2005. Experts workshop on Global Surface-based Network for long term observations of column aerosol optical properties, Davos, Switzerland, 8-10 March 2004. GAW report No. 162, WMO TD No. 1287, 153 pp.